Annals of R.S.C.B., ISSN:1583-6258, Vol. 25, Issue 5, 2021, Pages. 743-768
Received 15 April 2021; Accepted 05 May 2021.

Intelligent Approach for Skin Tumor Finding and Segmentation via Bivariate Shrinkage and Speckle Reducing Anisotropic Diffusion

D. Shanmuga Sundaram[1], K. Kavitha[2], Sathish Kumar .L[3], K. Thinakaran[4], Amudhavel .J[5]

[1]Assistant Professor, Department of Computer Science, H. H. the Rajah's College, Pudukottai - 622001, Tamil Nadu, India. dshhrc@gmail.com

[2]Assistant Professor & Head, Department of Computer Science, St.Justin Arts and Science College for Women, Cholapuram - 630557, Sivagangai. kavithakandavel88@gmail.com

[3]Assistant Professor, School of Computing Science and Engineering, VIT Bhopal University, Kothrikalan -466114, Madhya Pradesh. sathish.kumar@vitbhopal.ac.in

[4]Associate Professor, School of Computing Science and Engineering, Saveetha School of Engineering, SIMATS. thinakarank.sse@saveetha.com

[5]Assistant Professor, School of Computing Science and Engineering, VIT Bhopal University, Kothrikalan -466114, Madhya Pradesh. amudhavel.j@vitbhopal.ac.in

Abstract

Any irregular tissue development is called skin tumors. Malignant Melanoma and Basal Cell Carcinoma are among the most common forms of skin tumors. For the grouping skin lesions, the description and computation of various attributes like precise location, degree, form, and form is important. Advances of medical imaging technologies make diagnostic imaging a critical resource in medicine. For the clinical setting purpose magnetic resonance imaging, computed tomography, magnetic resonance angiography, and X-Ray angiography is frequently utilized. Computerized diagnostic execution is required due to the higher volume of clinical images and the recent developments in computing technologies that have rendered it possible to build these systems. For this research, we used the multivariate regression shrinkage added to the actual and complex noise reduction coefficients. The Speckle Reducing Anisotropic Diffusion (SRAD) helps to eliminate the noise after the reverse transition has actually occurred further to reduce the noise. This proposed system has been validated by various parameters like RMSE (Root Mean Square Error), PSNR (peak signal to Noise Ratio), PRD (Percent Residual Difference), (SSI) Structure Similarity Index and CCR (Correlation Coefficient are Related) to DTCW (Dual-Tree Complex Wavelet), CT (Curvelet Transform) and the WT (Wavelet Transform).

Keywords: Skin tumor Diagnosis, Melanoma, Wavelet transform, shift variance, divergence, fuzzy clustering, morphology, erosion, dilation, noise models

1. Introduction

Skin tumors develop as an outcome of the growth of single or multiple components of the tissue. Tumor cell image segmentation is really a key component of automatic radiographic medical diagnostics, and [1] studied cancer curvature. The pigments of the melanocytes that produce cells that are accountable for melanoma, a deadly type of cancer is increasingly generally around the

Annals of R.S.C.B., ISSN:1583-6258, Vol. 25, Issue 5, 2021, Pages. 743-768
Received 15 April 2021; Accepted 05 May 2021.

whole country. People may be rescued from this deadliest condition, as long as the illness is diagnosed in the initial phases so there is little spread. Dermoscopy is really a method that researchers use to analyze shifts in the skin with the aid of strong light and use distortion to minimize the glare of the air. The characteristic of melanoma with abnormal borders as mentioned in figure 1.

Fig 1: Abnormal skin growth sample

The wavelet sequence is a representation of an integral structure generated by wavelet that orthonormal sequence. A DWT is one where the wavelets are measured in a distinct way. The DTCWT utilizes simultaneous wavelet filters with directional help to handle the phenomena of shift variability and decays a picture into coefficients of complex and simple. The 3 higher-top filtering has contexts at 90 °, 0 ° and 45 ° in the actual two-dimensional filter rows, whilst the six subcarrier detectors are positioned at axes ±75 °, ±45 ° and ±15 ° for the complicated filters. The DTCWT [2] does have the benefit of strong directional specificity and hence is ideally reconstructed over the conventional Wavelet transformation. The bivariate shrinkage will be added to the modules at higher frequencies because the material elements are strongly influenced by the artifacts. The actual and theoretical modules are introduced jointly, and also to which bivariate shrinkage is added, the preserved sub-bands are defined after the removal of noise from such higher frequencies components. The SRAD [3] seeks to eliminate the noise speckle included in the clinical data. The SRAD is able to avoid splicing by altering valuable image details and losing sensitive picture edges by (IED) Inhibiting Edge Diffusion [4].

The entire research paper has been structured as follows: phase two describes the techniques applicable to the proposed method. phase three outlines the system specifics suggested, phase four interacts with BS (Bivariate Shrinkage) to model the figures on WC (wavelet coefficients), phase five introduces the SRAD Filter accompanied by FC in phase six, while phase seven introduces its empirical findings then, ultimately, phase eight ends the article with more work on the subject.

Annals of R.S.C.B., ISSN:1583-6258, Vol. 25, Issue 5, 2021, Pages. 743-768
Received 15 April 2021; Accepted 05 May 2021.

2. Related Work

The identification of skin cancers on clinical images is an important phase in the identification of cancers by the usage of clinical image segmentation techniques discussed by this [5] research article. Here clustering method has been used whereby identical artifacts are stored in different clustered and the correlation dependent on their levels of intensity is calculated. The clustering method has been used whereby identical artifacts are stored in different cluster methods and the correlation dependent on their intensity levels is calculated. Sensory Fuzzy-C clustering - based that causes their objects may respective concurrently too many groups, with various participation functions as experimented by [6]. Their methods of clusters will have the details dealing with by [7] on the skin tissue, cerebrospinal, white matter and cancer region. Pre-processing is necessary depending on the nature of the picture and common objects like distortion. Pre-processing is important to solve the issues that emerge with over classification. Deterioration and clotting for the replacement of unnecessary particles were done throughout the post-processing phase. A certain amount of cancerous cells and also the region of tumors could be estimated from the segmentation results. To determine the Sensitivity, Precision, and Consistency, the cancer segmented object is contrasted with the regular image. This may be noted that there is more consistency in the suggested procedure. When trying to diagnose the cancer region, the picture quality needs to be improved because it is influenced by the noise that may render it challenging to interpret valuable details. Literally, the classification objective is to find out the cancer region and to decrease the negative impacts as often as practicable so the picture transform is completed. The key goal, however, is to raise RMSE and PRD and also PSNR, SSI, and CC. It contributes to correct tumor region estimation and therefore is more precise the prediction of skin cancer. It is possible to estimate the distribution belongs to the last scan in the cancer region.

- ✓ Beaver's contraction minimizes noise.
- ✓ Decreasing Speckle eliminates DBS's The Starburst Pattern Disturbed in the clinical Visual Image.
- ✓ DTCWT eliminates artefacts that conventional wavelets throughout restoration
- ✓ Using this process the better signal to noise Level could be obtained.
- ✓ The mutual information Factor seems to be so much thus the resemblance among the opposed image and feedback becomes more pronounced as the distortion is mostly entirely reduced.
- ✓ Reduces the proportion of remaining variance and diskettes standard errors.
- ✓ Evaluate Volumes of Tissues
- ✓ Planning for Surgery
- ✓ The immediate examination with strokes
- ✓ Identifies cancers as well as such pathologies then treat intraoperatively

Annals of R.S.C.B., ISSN:1583-6258, Vol. 25, Issue 5, 2021, Pages. 743-768
Received 15 April 2021; Accepted 05 May 2021.

3. Proposed Method

Skin tumors are disorders whereby cancerous cells throughout the skin texture membranes begin to develop. This is because cancers are irregular cell development in the blood. While these growing are usually known skin cancers, tumors are not one of the skin tumors. The skin tumor is the exact opposite of malignant.Tumor cells require a blood supply to stay alive, as do all cells in the body. The tumors that don't invade or expanded adjacent tissues to faraway areas were also named innocuous. A cancerous lump is usually quite serious than like a malignant. Nonetheless, a cancerous lump may also cause certain skin complications by pulling on surrounding cells. Visual pictures are sensitive to a wide host of object classes. Noise is the product of errors in the phase of image processing resulting in neighboring pixels that do not represent the actual intensity values. Typically the visual pictures are influenced by the noise signal called the vector Noise and a cumulative noise named the starburst pattern Noise.

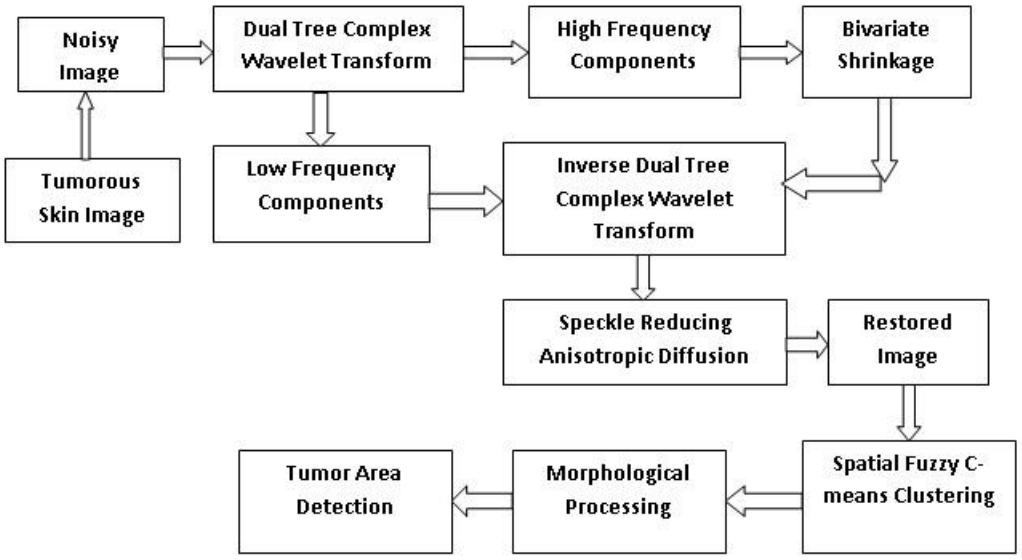

Figure 2: Proposed DTCWTsystem architecture

The design of the conceptual device is seen in fig 2. It takes the form of a Fourier transform, the multivariate regression slippage, the spatial domain reducing blurriness as well as the clustering of Fuzzy C-means that are the major frames of this scheme.

3.1 Dual Tree Complex Wavelet Transformation

The word wavelet relates to a time-limited oscillating disappearing phase which has the potential to define the frequency domain axis, with elements of various period assists. We provide an important method for evaluating non-stationary or transitory anomalies. Wavelets are really a statistical method for extracting knowledge from several forms of data, like acoustic input.

Annals of R.S.C.B., ISSN:1583-6258, Vol. 25, Issue 5, 2021, Pages. 743-768
Received 15 April 2021; Accepted 05 May 2021.

Arithmetically the wavelet is a slowly varying feature, with the value distributed in period and defined in following equation 1.

$$\int_{-\infty}^{\infty} \Psi(t)dt = 0$$

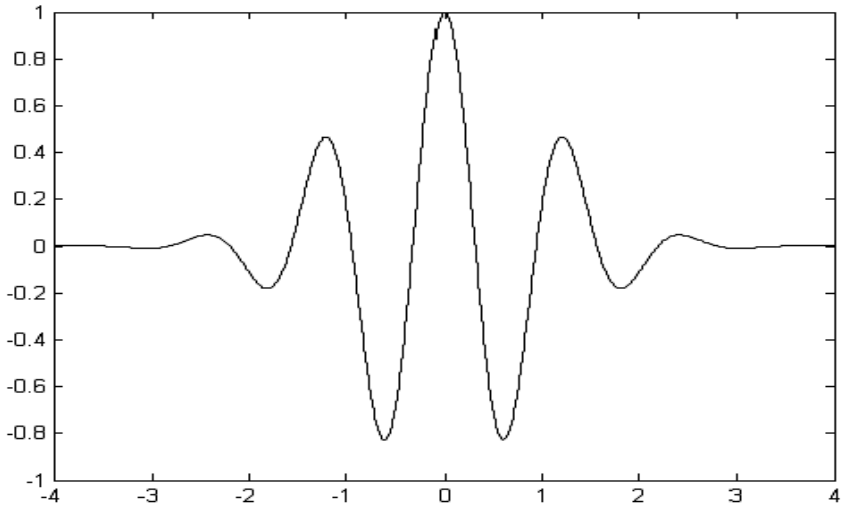

Fig 3: A simple wavelet representation

In addition to become further efficient in the extraction of spatial – frequency data, a wavelet community can be built from a method Ψ (t) that is also recognized as the mother wavelet, restricted in a given field. The Daughter Wavelets, Ψu,s(t) are established by a component u transcription and a typically categorized s clotting as in following equation 2.

$$\Psi\_(u,s)\ (t)= \ 1/\sqrt{s}\ \ \Psi((t-u)/s)$$

The validation of wavelet is justification measures shows on the wavelet method the signal to be analyzed. It is mention clearly the following equation 3.

$$\langle x(t),\Psi\_(u,s)\ (t)\rangle= \int\ [\![x(t)\ \Psi\_(u,s)\ (t)dt]\!]$$

The DWT has characteristics such as strong signal energy reduction, complete restoration with limited filtering service, no duplication, and quite weak computing. Despite the excellent properties of actual wavelets, some common problems exist, these are represented in table1.

Table1: Comparisons of wavelet properties

Lack of directionality	Multidimensional correlations of the wavelet generate a sequence which is directed in many ways at the same time.
Oscillations	Wavelets were also processes of the bandpass filter; therefore their correlations fluctuate positively and negatively around singularities.
Aliasing	Aliasing is made by computing the wavelet constants by reducer

Annals of R.S.C.B., ISSN:1583-6258, Vol. 25, Issue 5, 2021, Pages. 743-768
Received 15 April 2021; Accepted 05 May 2021.

	processing period, testing upwards operational activities.
Shift variance	Wavelets will fluctuate by a frequency response change around the singularities.

Problems with the DWT are overcome by the property of the frequency domain. Fourier series, unlike with the DWT, doesn't suffer from the described issues. The evaluation of the frequency domain is based on multiple weighted oscillatory ventricles and defined in figure 5.

$$e^{j\Omega t} = \cos(\Omega t) + j\,\mathrm{Sin}(\Omega t)$$

The oscillating central consequence (cosine), as well as imaginary part (sine) structures, comprise a Hamilton transformation combination that generates an empirical emission signal $e^{j\Omega t}$ that is only assisted on half of a time spectrum (W > 0). The CWT with complicated, remunerated implementing organizational could be provided on the basis from the above recognition as in the formula:

$$\Psi c\,(t) = \Psi r\,(t) + j\,\Psi i\,(t)$$

According to the above formula, Ψr(t) is genuine and then even and ubiquitous and ubiquitous and by creating the Hilbert incorporate set they end up making ubiquitous Ψc(t) as an analytical signals. The wavelet transform tree signals x for an input 1D. Within it can be seen respectively the real and imaginary portions of the inputs and outputs. A wave tree with a complicated 1D can be seen in fig 4.

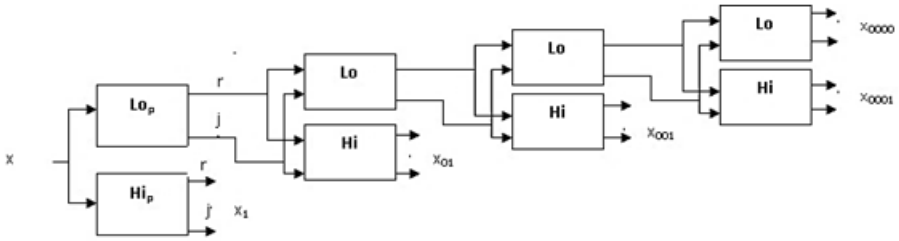

Figure4. Complex wavelet tree

The expansion of specific wavelet transform to 2D is accomplished by separable sorting into rows and columns afterwards. The figure 5 has represented wavelet transform tree has two stages.

Annals of R.S.C.B., ISSN:1583-6258, Vol. 25, Issue 5, 2021, Pages. 743-768
Received 15 April 2021; Accepted 05 May 2021.

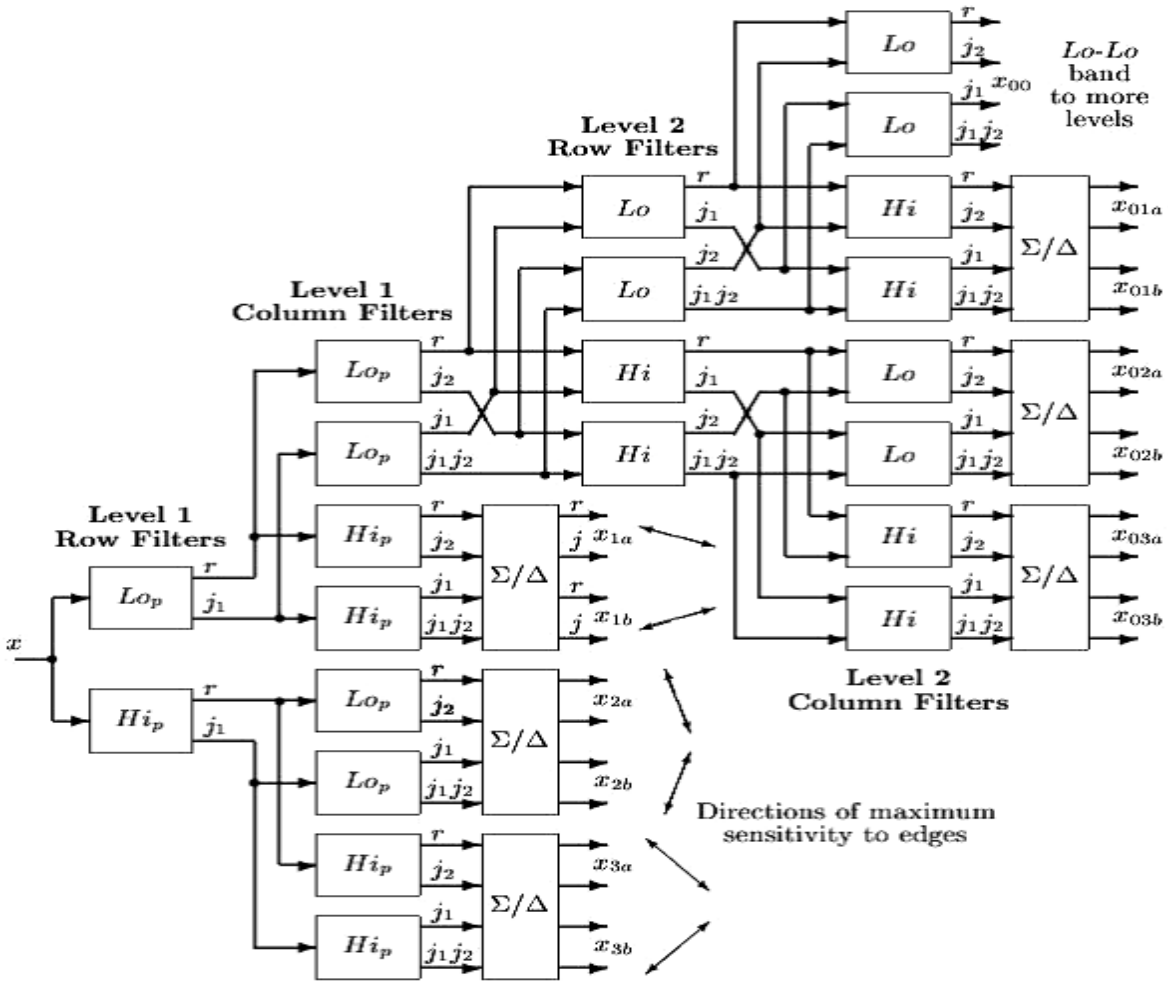

Figure 5: 2D tree view of Wavelet

True weighted wavelet filters throughout the DTCWT generate the hypothetical part of a transformation in simultaneous trees for decomposition. The key benefit of a DTCWT would be that the decomposition happens with a significantly greater level of directional cues than conventional DWT lacks.The individual weighted pixel values are substituted by scaling function coefficients with a suitable system design that meets the necessary refinement requirements as deal with this by [8]. Therefore the complex filter could be broken into three positive real filters respectively.The complicated filters would then be broken into three positive real filters again. Thereby, the Hilbert regenerate set is formed by two positive real filtration which offers their corresponded frequency components in quaternion, which is considered as just an analytical filtration handled by [9].

The Two dimensional DWT generates 3 orientation judicious sub-band for every stage articulating representations features image-oriented at 95o, ± 49o, and Zero directions, while the Two-dimensional DTCWT generates 6 axis sub-bands for every stage to reveal object info in ±16o, ± 46o, and ± 76o directions, in addition to the data acquired from DWT particular angle.

Annals of R.S.C.B., ISSN:1583-6258, Vol. 25, Issue 5, 2021, Pages. 743-768
Received 15 April 2021; Accepted 05 May 2021.

Two-dimensional DTCWT implementing comprises of 2 phases.First of all, 's diversified Two dimensional DWT divisions disintegrate an input data to a desirable size, which filtering was precisely built to satisfy the Hilbert pairing specification and for each process includes high-pass and sub-bands are produced.ABx, AAx, ABy, BAy, AAy and BAx. Secondly, whether by combining or differentiating, every two equivalent sub-bands that have the same carry-bands are merged sequentially. As a consequence, Two-dimensional DTCWT sub-bands were produced for each point utilizing in the following Equation.

$$((BA\_x+BA\_y))/\sqrt{2}\ ,((BA\_x-BA\_y))/\sqrt{2}\ ,((AB\_x+AB\_y))/\sqrt{2}\ ,$$

$$((AB\_x-AB\_y))/\sqrt{2}\ ,((AA\_x+AA\_y))/\sqrt{2}\ ,((AA\_x-AA\_y))/\sqrt{2}$$

The 6 wavelets clearly mentioned above have the orthogonal were the sum of difference process, which represents a complete transformation of the restoration wavelet. Two-dimensional DTCWT's fictional component has an identical base process to the true component.The bandpass filter has 6 intricate high-pass and sub-bands at every point, and two intricate low-pass and sub-bands, as opposed to 3 real high-passes and one true low-pass and sub-band for both the actual 2D transformation. The Wavelet Dual Tree Intricate Transformation has been represented in figure 6.

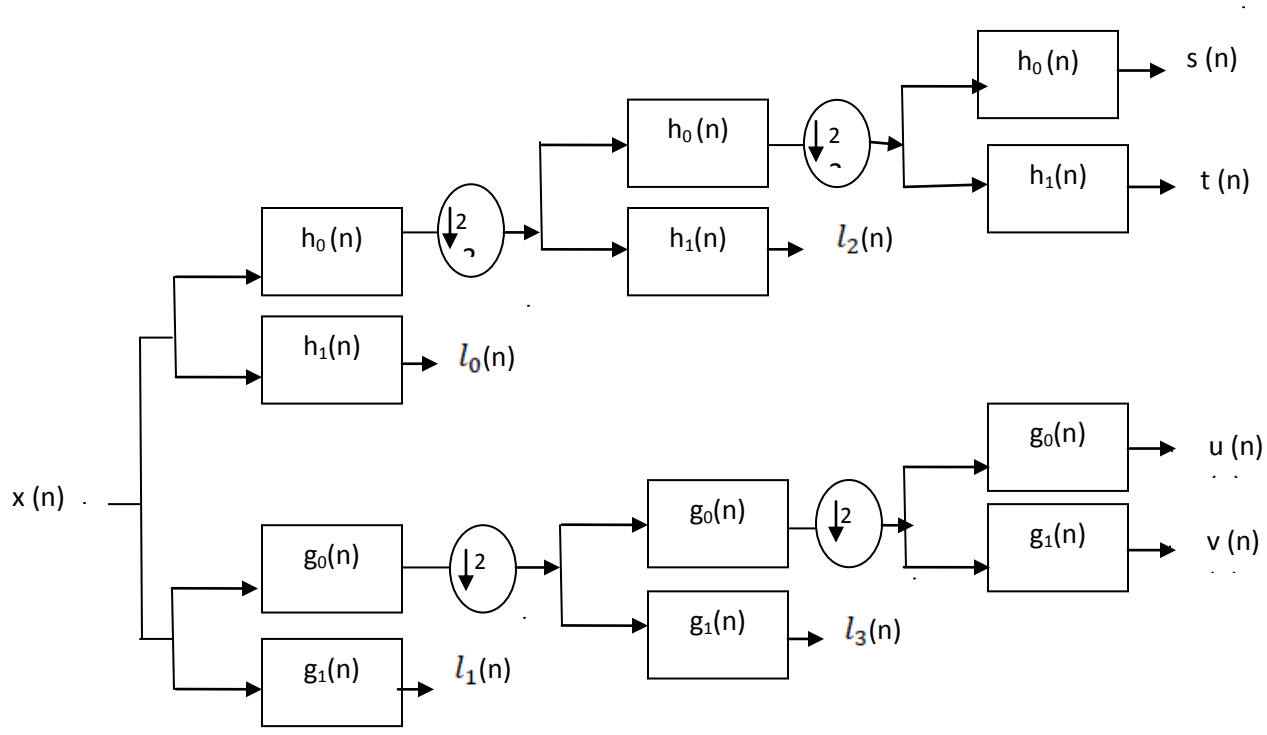

Fig 6: The Wavelet Dual Tree Intricate Transformation

Annals of R.S.C.B., ISSN:1583-6258, Vol. 25, Issue 5, 2021, Pages. 743-768
Received 15 April 2021; Accepted 05 May 2021.

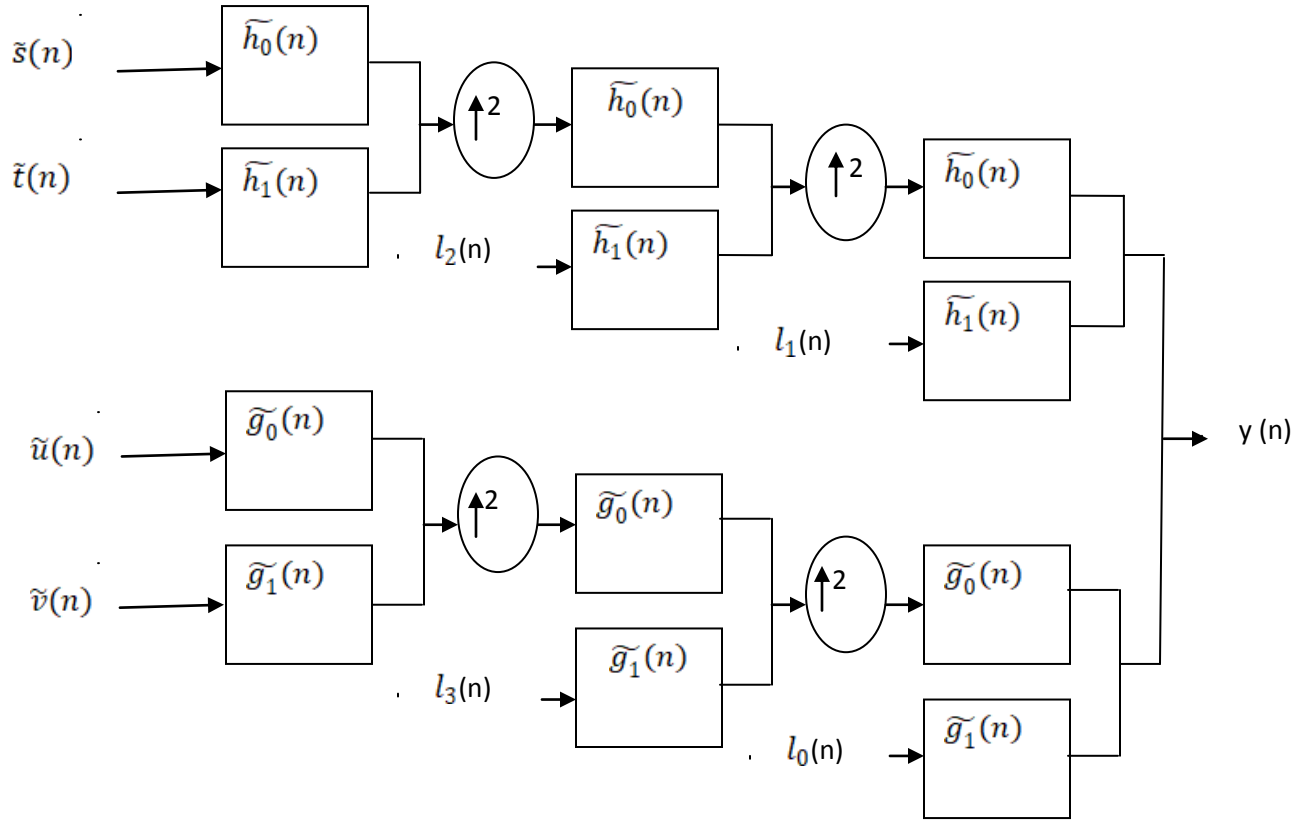

Fig 7. The Contrast Wavelet Dual Tree Intricate Transformation

4. BS (Bivariate Shrinkage)

The BS is a modern completely non Gaussian bivariate probability distribution method for modeling clinical image wavelet scenario. The approach incorporates the coefficient of dependency between such a wavelet as well as its parent method. The altered BS function that relies on both the coefficient and its parent method yields enhanced findings for de-noising wavelet dependent image.In the method of BS the shrinkage would be larger for lower parental method value. A locally adaptive threshold de-noising approach is derived from of the BS method, and it has been clarified in this research article [10].For increasing WC (wavelet coefficient) it SB methods needs previous understanding of the noise variability and the signaling variability.In order to calculate the BSC (Bivariate Shrinkage Coefficient), a prior knowledge of both the noise variable, σ_n*n and the residual variance, by every wavelet function, should be given. The residual variability for Rth is calculated using adjacent parameters in field M(R).Here M (r) is described like all variables inside a square-shaped period that's also shrunk only at factor Rth.

Annals of R.S.C.B., ISSN:1583-6258, Vol. 25, Issue 5, 2021, Pages. 743-768
Received 15 April 2021; Accepted 05 May 2021.

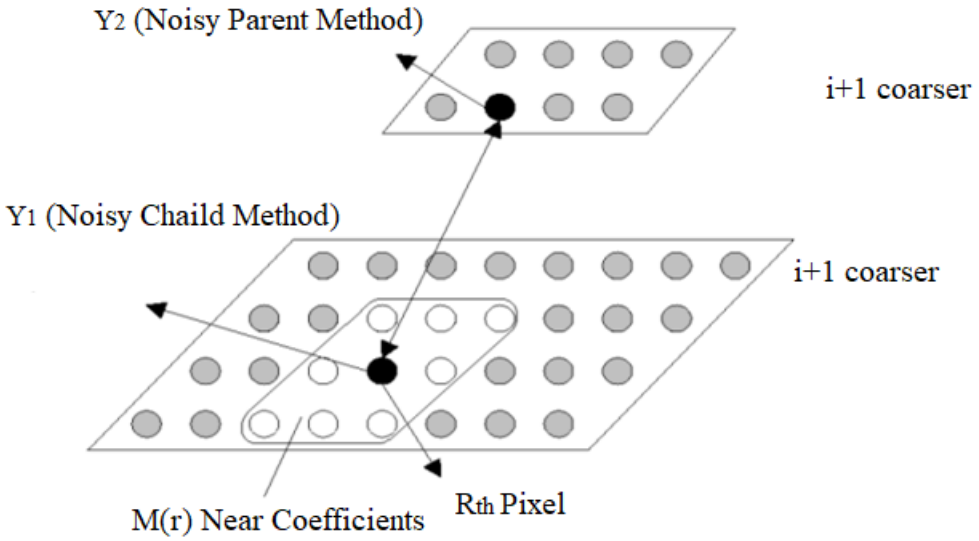

Fig 8. Neighboring co-efficient analysis

The approach calculates the noise variability initially, then the signal variant, and calculates each coefficient to use the SB function of the bivariate. The σ_n^2 tomeasure the noise variability, a reliable average estimation method from the best WC is used to measure the noise variability. It was shown in following equations.

$$\text{Noise Variance, } \sigma_n{}^2 = \frac{\text{average } (x_i)}{0.632}$$

It is ok for the residual variability of noisy measurements x_1 and x_2 to approximate the marginal deviation for the R_{th} WC, but it is referred said as σ_m*m. Although h1 or rather h2 are constructed as a negative average, the following formula can be used to obtain σ_h*h.

$$\sigma_x^2 = \frac{1}{N} \sum_{x_i \in M\,(r)} h_i^2$$

Where, N = Size of the neighbourhood, M (r).

The residual deviation $\sigma^2$was its amount of the noise variability σ¯m*m as well as the residual variability of the noise measurement σ_x*xwas measured and is defined in the following equation.

$$\sigma_x^2 = \sigma^2 + \sigma_m^2$$

The meaning of σ can be derived from of the aforementioned formula as shown as below equation.

$$\sigma = \sqrt{\sigma_x^2 - \sigma_m^2}$$

Annals of R.S.C.B., ISSN:1583-6258, Vol. 25, Issue 5, 2021, Pages. 743-768
Received 15 April 2021; Accepted 05 May 2021.

The magnitude of the limit, the H is calculated using variability of noise, σ_m*m as well as the variability of the signal, σ^2. Just let measurement of the distance of double tree complexes is represented as ws0. Through which could be calculated the BSC S_0 with the following formula.

$$S_0 = \begin{cases} ws_0 - H & ; if ws_0 > H \\ 0 & ; if ws_0 < H \end{cases}$$

5. SRAD (Speckle Reducing Anisotropic Diffusion) Filter

To speckled pictures, Bivariate Speckle Reducing Anisotropic Diffusion is the edge or boundary-sensitive propagation, even like traditional boundary detection is the advantage boundary sensitive diffusion for clinical image tainted by noise signal. To avoid noise while missing major sections in a clinical image such as boundaries and outlines or certain information are nonlinear and distance variants style filter.This is boundary-sensitive PDE expansion of the evolutionary speckle which reduces filters such as Frost and Lee. The propagation cycle participating two controllers, i.e. crews with gradients and divergences. It's also calculated by seeking saturation function component separation, and curve equivalents.For two variables like starburst pattern economic limit (W0), and immediate coefficient value of variance (W), the saturation coefficient decides. The role W serves in the speckled analogy as boundary detector that shows high elements at boundaries and less value. As well as the W_0 feature determines how much adaptable is added to a clinical image.The upgrade method for diffusion is illustrated in the following Equation.

$$V^{i+1} = V^i + (T/4) * G^i$$

Where, V^{i+1}– Space outcome,

i– Input of noisy,

T = Time iterated by 0.5,

G^i–Dispersal method.

While the latest DE speckle filter is named boundary preservation and aspect preservation, the sorting technique has significant shortcomings. Second, the filters were sensible of the filter frame size and form. Too much-smoothing can arise due to a filtered image which is too wide so boundaries may be blurry.A narrow aperture diminishes the filter's smooth potential and removes the starburst pattern. Third, current filtering may not boost boundaries, but they prevent relatively close-edge mapping. Second, the filters with DE speckle really aren't longitudinal.

Because of the filter frame area and structure as defined by [11], the Partial differential equation dependent speckle separations approach enables the creation of an object scale-space beyond

Annals of R.S.C.B., ISSN:1583-6258, Vol. 25, Issue 5, 2021, Pages. 743-768
Received 15 April 2021; Accepted 05 May 2021.

bias. Why does SRAD protect boundaries but that also strengthens boundaries by hindering edge propagation and facilitating migration from either part of the point. SRAD is flexible and cannot use hard limits in order to adjust output in homogeneous areas, areas neighborhood too edges, and smaller objects. SRAD may maintain its boundaries and even boost its edges; however, this feature is strongly reliant on edge detection precision. Unless the edges also aren't identified, it does not strengthen the edges and or soften it.And if the noise is perceived as borders, therefore the noise won't be softened or even decreased. The benefits of anisotropic propagation entail trying to smooth throughout the based on inter-region and boundary protection. For artifacts distorted by frequency components, anisotropic reduction works very well.

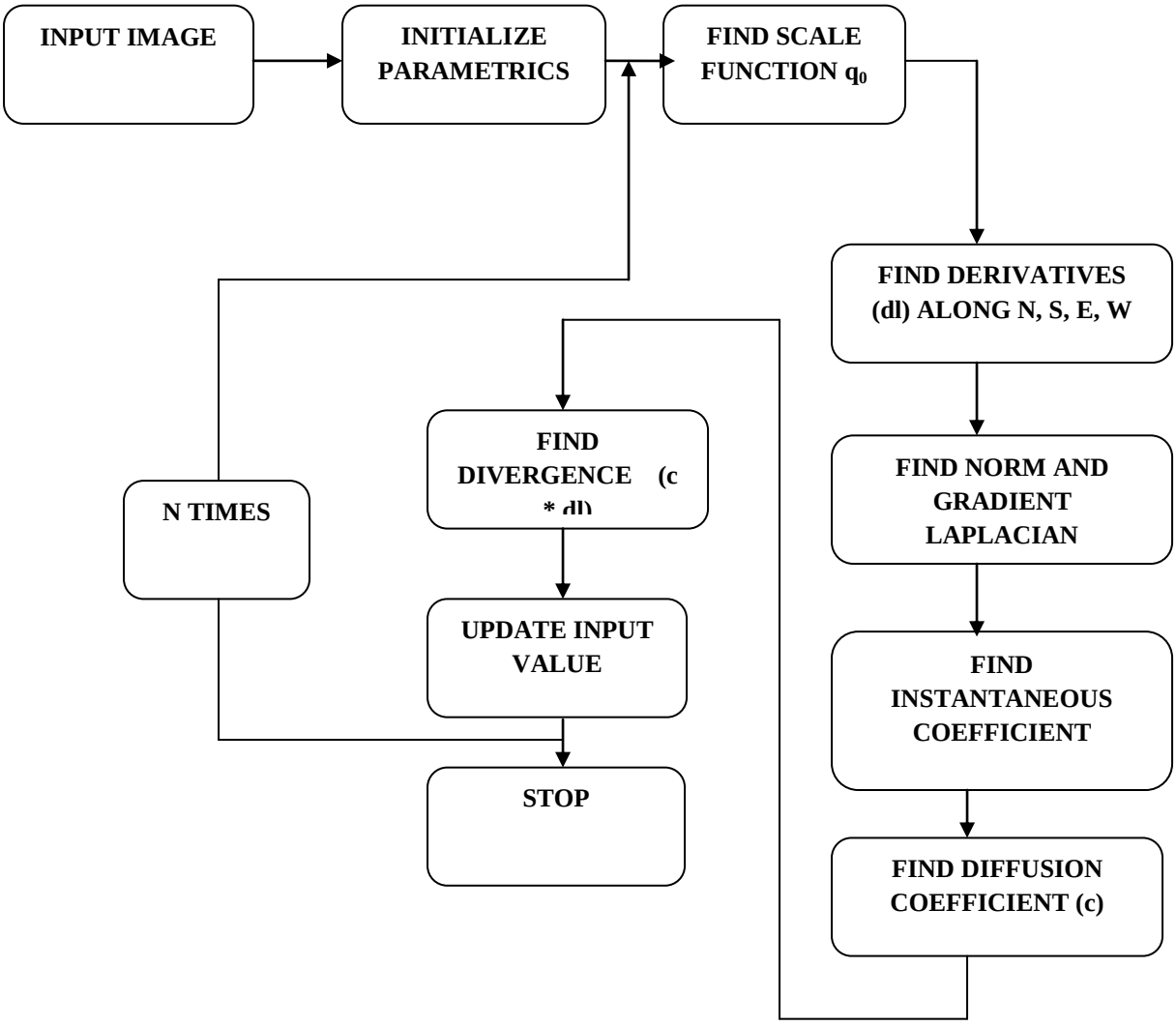

Fig 9. Architecture of Speckle Reducing Anisotropic Diffusion

6. SFC (Spatial Fuzzy Clustering)

The FC (Fuzzy Clustering) has a significant role in problem-solving in pattern identification and blurred object analysis fields. A number of FC approaches were suggested and many are focused

Annals of R.S.C.B., ISSN:1583-6258, Vol. 25, Issue 5, 2021, Pages. 743-768
Received 15 April 2021; Accepted 05 May 2021.

on range parameters as defined by [12].Another utilized often method was its function Fuzzy C_f implies. To measure weights of fuzzy it requires inverse space. The updated FCM is one very efficient technique. It uses Gaussian weights as defined by [13, 14] to measure the clusters core.Spatial Fuzzy C_f tends to mean approach combines location data, but every group's membership ranking is changed based on near are pixels as handled by [15] and [16]. The very first step for determining the membership variable in the latent space is much like the in regular FCM.The first step for determining the membership property throughout the spectral method is much like the regular FCM. Throughout the second viewing, every other pixel element membership data is connected to the spatial field, and from the spatial method is calculated. The FCM version has also been defined by [17] and [18] with both the new participation that is integrated with the spatial methods.

The initialization of the FPM (Fuzzy Partition Matrix) originally occurs. The ranking is initialized with the use of features extracted or by chance. The initialization method for the FPM is performed completely at random, as well as its size should be equivalent to the number of groupings and the width of the image as rows or columns respectively.

Secondly, the participation function is calculated from the FPM initialized like in following formula.

$$\mathrm{MF} = \frac{FPM}{\sum FPM}$$

Finally, the middle becomes calculated at each group depending on the strength of an input part of image and the MF calculated using the following Formula.

$$\mathrm{Middle} = \frac{\mathrm{MF} * \mathrm{Input\ Img.}}{\sum \mathrm{MF}}$$

Next, it calculates the distance by determining the difference between all the middle and the pixel input. This same length in the scheme is expressed in following equation.

$$\mathrm{Length} = \mathrm{abs}\ (\mathrm{Pixcel\ Input} - \mathrm{Middle})$$

Revised MM (Membership Matrix) is eventually to be decided. Altered MM is inverse linear to Euclidean length square and will be modified through repetitions. The SFC flow diagram as represented in following figure 10:

Annals of R.S.C.B., ISSN:1583-6258, Vol. 25, Issue 5, 2021, Pages. 743-768
Received 15 April 2021; Accepted 05 May 2021.

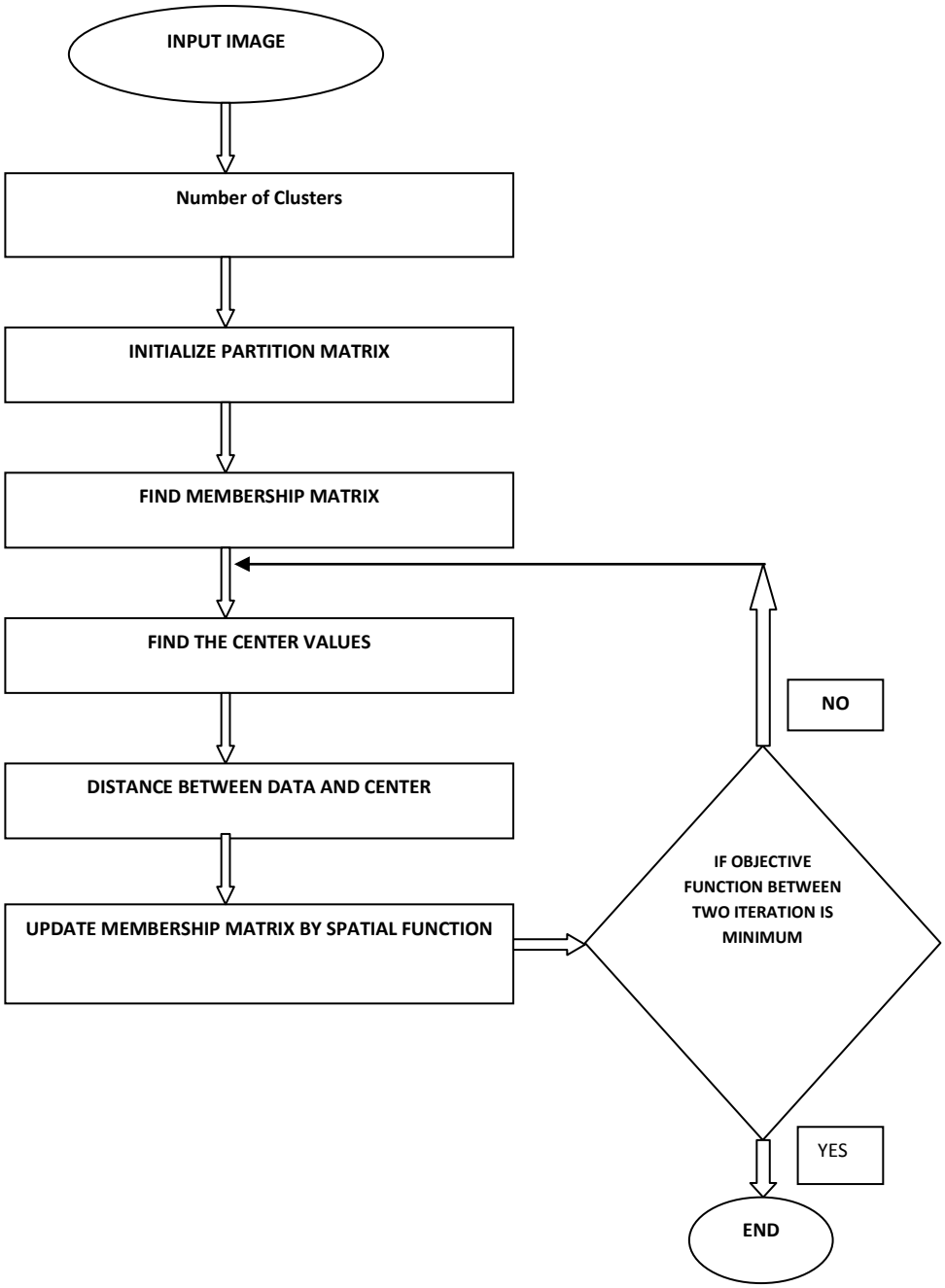

Fig 10. FSC Architecture

Grouping is an important strategy in transfer classification. Fuzzy C_fMeans grouping is a well-known method of soft segmentation and is most suited for segmentation of medical images. Nevertheless, this modern technique is determined by reducing the difference between both the pixels input or image and the cluster point's recursively.Spatial adjacent pixel association is an aid to the segmentation of images. Such adjacent pixels are strongly correlated and therefore have similar image features information. Most pixels on an image are strongly correlated, i.e. this same pixel values in the local vicinity might have the same data on the features.

Annals of R.S.C.B., ISSN:1583-6258, Vol. 25, Issue 5, 2021, Pages. 743-768
Received 15 April 2021; Accepted 05 May 2021.

Therefore, neighbor pixels' structural association is a significant characteristic for improving FCM efficiency as defined by [19].Clustering strategies are often unsupervised approaches that could be used to arrange input objects into various based on the similarity between the specific pieces of data. The Fuzzy C_f Means algorithm is an incremental algorithm that seeks clusters in information so this utilizes the definition of the fuzzy set.Cost reduction is achieved by assigning high membership variables to pixels closing to just the centroid of their clusters methods and assigning low absolute value to pixels with information far outside the centroids. The membership component represents the likelihood of a pixel belonging to a cluster in question.Another of the issues with regular FCM in the segmentation of images is the absence of spatial data. Although the noise of image and artifacts also impair FCM segmentation efficiency, since neighbors pixels have equivalent feature values, and the likelihood of belonging to the same cluster is high so it would be desirable to include spatial data in a standard FCM approach.The FCM approach minimizes the speckle noise since there is no same cluster in the region, the size of the noisy group is reduced significantly with FCM that is not the case with K means was defined by [19]. Additionally, the cluster distribution in the neighboring pixels enhances the membership of the correct cluster.

6.1 Morphological Process

Anatomical image segmentation is a set of non-linear procedures that have to do with the structure or anatomy of image features. Segmentation algorithms for morphological computations depend primarily on the similar sequence value of image pixels, not really on their data variables, and are thus particularly well suited to binary computer vision for images.Morphological strategies investigate an image named a formulating feature with such shape as small or prototype. The structuring factor is located in the picture at all potential locations but is contrasted with the respective pixel locality. Several operations evaluate whether the feature fits inside the neighborhood, whereas others evaluate whether it meets the neighbors or overlaps and describes.Where similar ellipse is also an ellipse in the last formula, which has the same angular velocity as the feature extraction picture taken in. Nearly 76.6 per cent of skin tumors are identified as malignant with aid of the above mentioned mitigated test.The (GA) Geometric Asymmetry could be determined by splitting the skin tumor to two sections by a horizontal path that signs through the middle of weight, posting a contrast between separated into two sections by measuring the length between both the components of the dimension. This also determines the importance of qualitative asymmetry. That probe of an image with a structuring feature is included in the in figure 11.

Annals of R.S.C.B., ISSN:1583-6258, Vol. 25, Issue 5, 2021, Pages. 743-768
Received 15 April 2021; Accepted 05 May 2021.

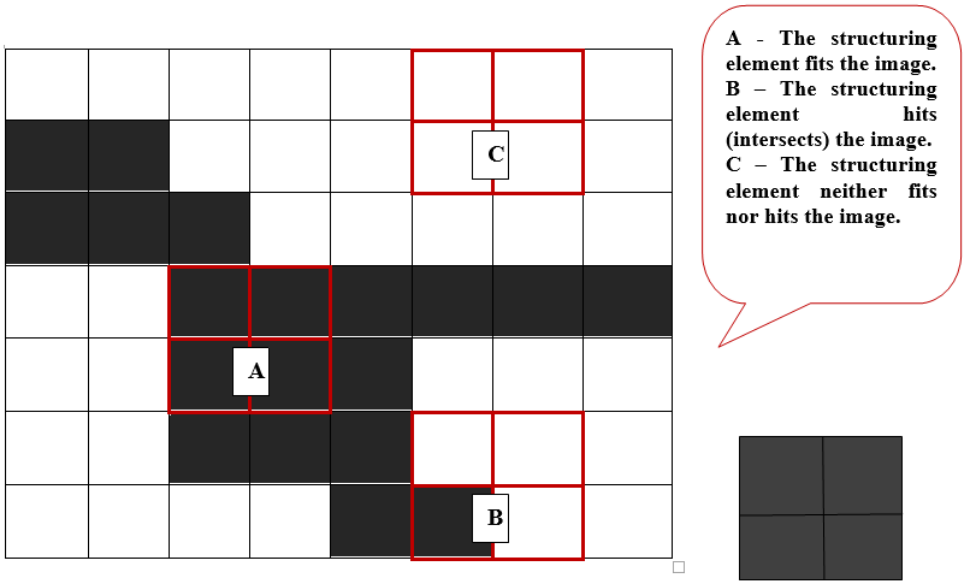

Figure 11. Fig 11: Probing of an Image with a Structuring Element

A morphological experiment on a binary image produces a new binary image wherein the pixel has a nonnegative value unless the measurement at a certain position in the source images is successful. The formulating factor is a low binary, that is to say, a small pixel size matrix, every with 0 or 1.Wherein, the length of the input image is defined by the vector dimension. The formulating unit structure is determined by the pattern of 1 and 0. Any of the pixels is typically a source of the intensity value, but normally that source may be outside of the intensity value. Specimens of the texture features are seen in Figure 12.

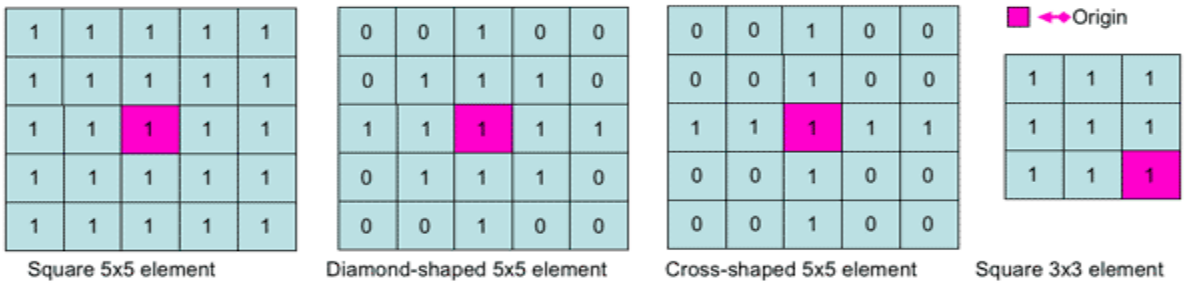

Fig 12: Structuring elements examples

A common concept is to have odd structuring matrix measurements or the filed specified as the matrix center. By putting a transformation function in a binary image, every one of the pixels its organizing component is identified with the respective pixel of a neighborhood.The constructing factor is said to match the image if the respective pixel value is 1 each of its pixel set to 1, likewise, another object is shown to touch or overlap a constructing feature if the respective set pixel value is minimum one.

Annals of R.S.C.B., ISSN:1583-6258, Vol. 25, Issue 5, 2021, Pages. 743-768
Received 15 April 2021; Accepted 05 May 2021.

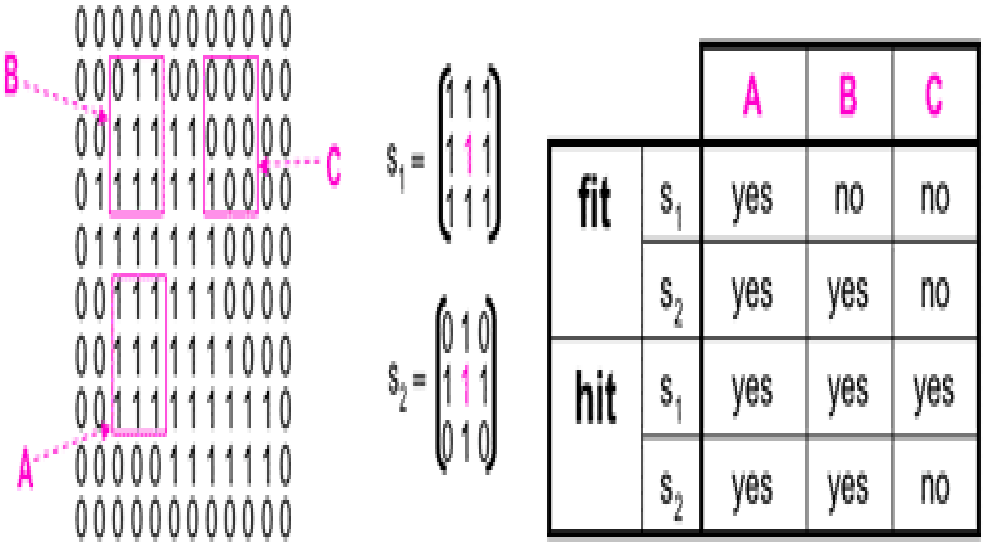

		A	B	C
fit	s_1	yes	no	no
	s_2	yes	yes	no
hit	s_1	yes	yes	yes
	s_2	yes	yes	no

Fig 13: Fitting and hitting

6.2 Erosion and Dilation process

The degradation of a binary image *f*by such a formulating element s results inside a fresh binary image *B = Fr xnors* for all at certain positions of a source of a transformation function at which the constructing component *s* fits the picture *Fr* data. The holes and gaps between various regions are becoming bigger, removing small data; it was clearly represented in figure 14.

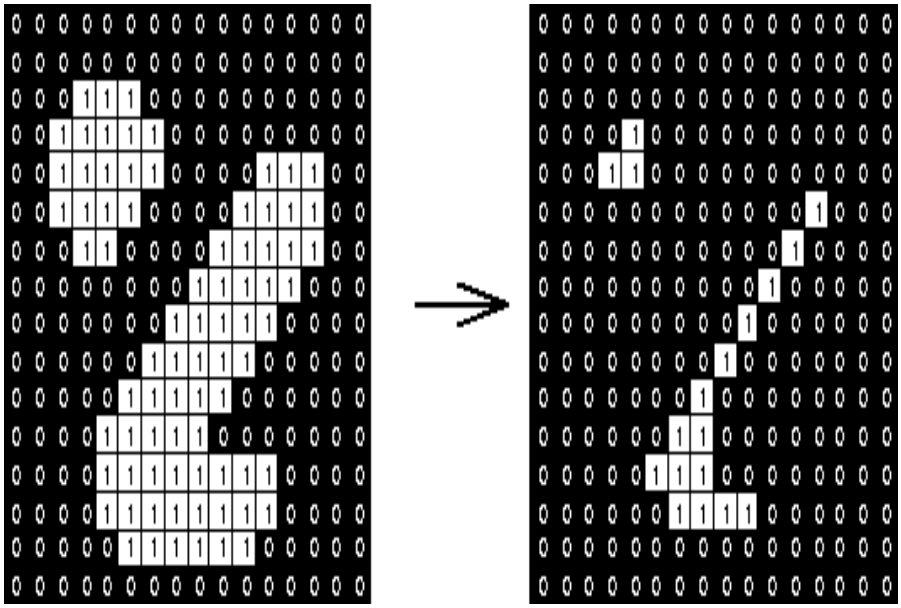

Fig 14: Erosion using a 3x3 square structuring element

Annals of R.S.C.B., ISSN:1583-6258, Vol. 25, Issue 5, 2021, Pages. 743-768
Received 15 April 2021; Accepted 05 May 2021.

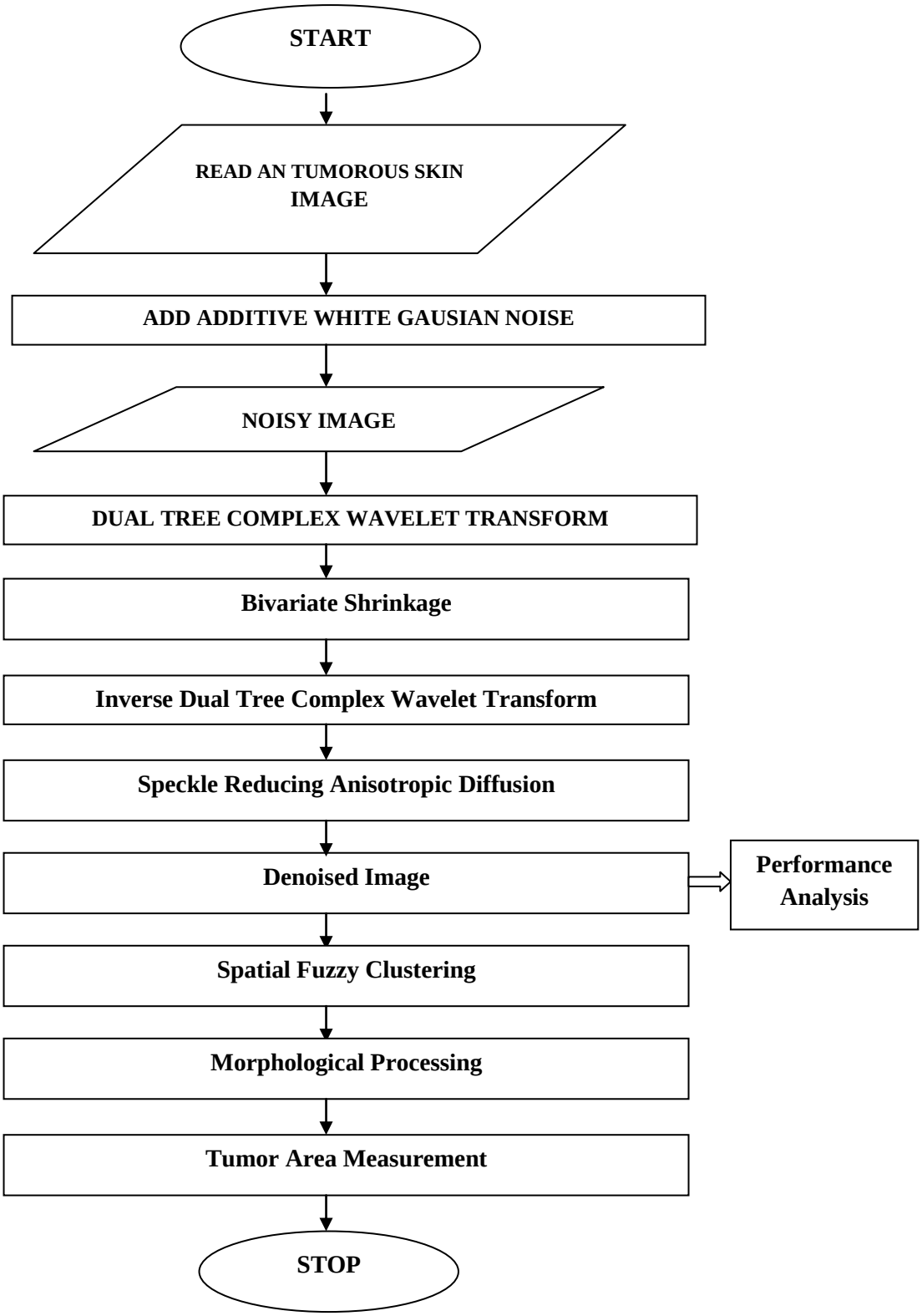

Fig 15: Flow chart of the proposed method

Annals of R.S.C.B., ISSN:1583-6258, Vol. 25, Issue 5, 2021, Pages. 743-768
Received 15 April 2021; Accepted 05 May 2021.

Bigger constructing components have a much more noticeable effect, as the outcome of attrition with a broad transformation function is identical to obtained results from iterative process attrition with a small intensity value of the same type. Erosion extracts small-scale information from a binary picture but at the same time decreases the size of involved areas.

The edema of an image Fr through a structuring component s creates a binary image specified by $H = g\ xor$s with those at both positions of an origin structuring component where the structuring component *s* reaches the provided input image *Fr* pixels.

Dilation provides the opposite result to displacement, which implies that the inner and outer borders of areas are connected to a sheet of pixels. The spaces surrounded by a single area and the differences between various regions are getting narrower, and minor intrusions it into area 's borders are filled; it has shown in figure 16,

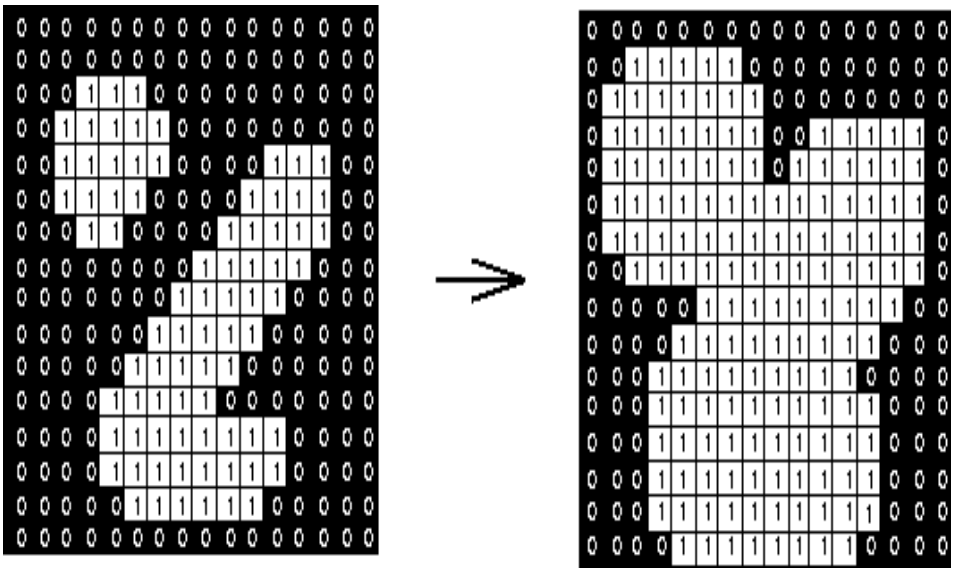

Fig 15: Dilation using a 3×3 square structuring element

This same dilation or erosion effects are determined by either the size or shape of a constructing item. Deformation and degradation are parallel activities such that the results are the opposite.

When a binary image is assumed to be a series of attached pixel areas fixed to One on a pixel backdrop fixed to Zero than erosion was its adjustment of a structuring component to these borders as well as dilation was its adjustment of a structuring component to the past, accompanied by a reversal of the effect.

Dilation is, in basic terms, the method of inserting a pixel at the boundary of the site depending on the structuring feature. The definition for identifying output pixels is a cumulative neighborhood matrix of the input pixels. Deterioration is based mostly formulating factor that detach the pixel from edge of an entity. Finally the resulting picture is smoothed to minimize context blur and sharpness of the edge.

Annals of R.S.C.B., ISSN:1583-6258, Vol. 25, Issue 5, 2021, Pages. 743-768
Received 15 April 2021; Accepted 05 May 2021.

7. Experimental Results

Throughout this study, we suggested using the BS process, which is a modern basic Non-Gaussian bivariate wave equation activity that helps design image statistics of wavelet. It is accompanied through Bivariate SRAD, a unique filter for eliminating the added noise and for retaining the borders.It is also provided to accurately detect the skin tumor fields of clustering based as well as morphologic analysis. The techniques suggested were applied to a collection of 410dermoscopic photographs of different sizes given by healthcare professionals. This set includes all forms of skin cancer, including healthy lesions.

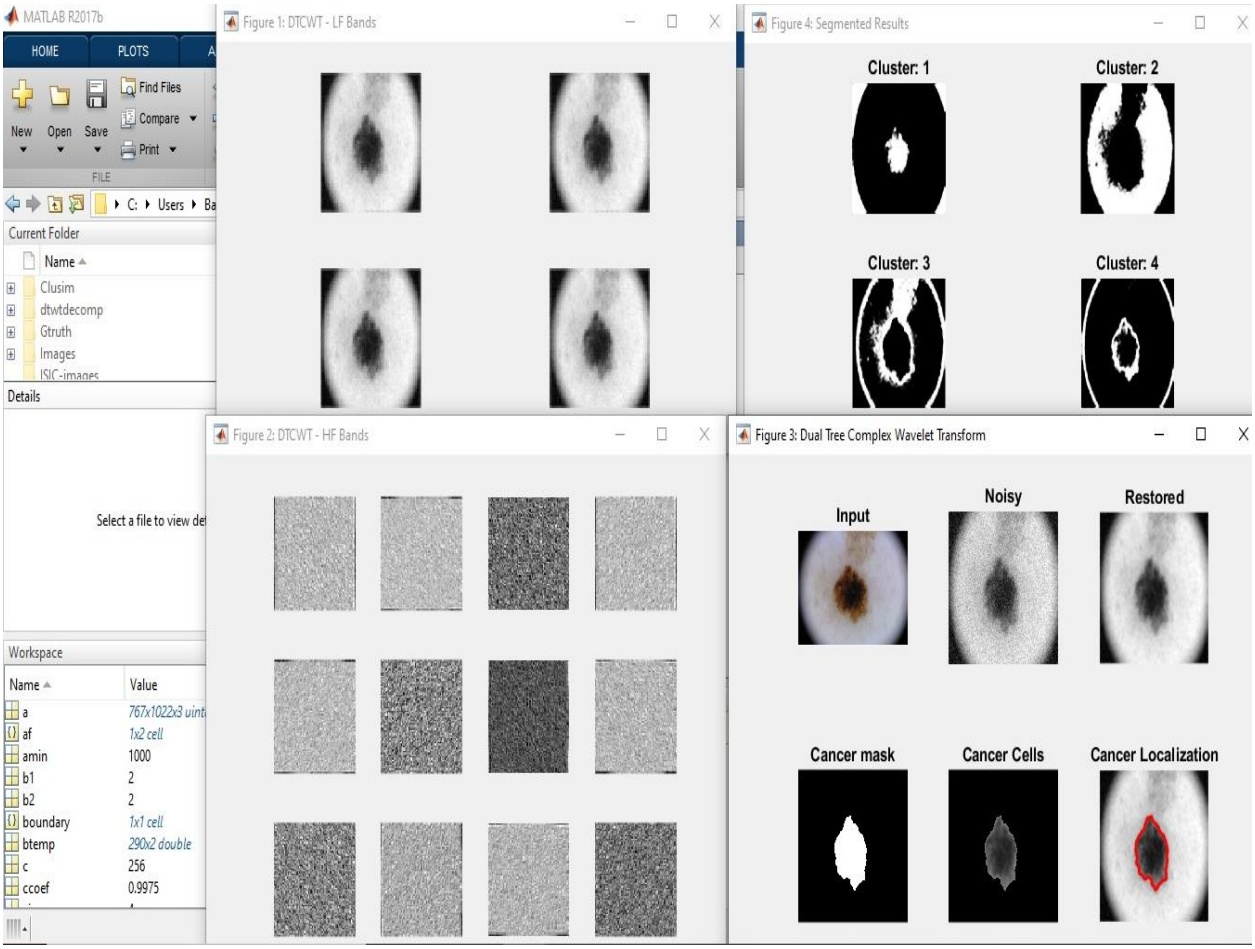

Fig 16: DTCWT LF bands (Left top), HF bands (Left Bottom), Cluster outputs (Right top) and cancer localization (Right bottom)

We have utilized MatLab for Image processing along with wavelets simulator. We receive the source signals DWT duration 16 scale filters.

Figure 17 indicates another experimental production that has more added noise and is successfully handled with the current process of filtration.

Annals of R.S.C.B., ISSN:1583-6258, Vol. 25, Issue 5, 2021, Pages. 743-768
Received 15 April 2021; Accepted 05 May 2021.

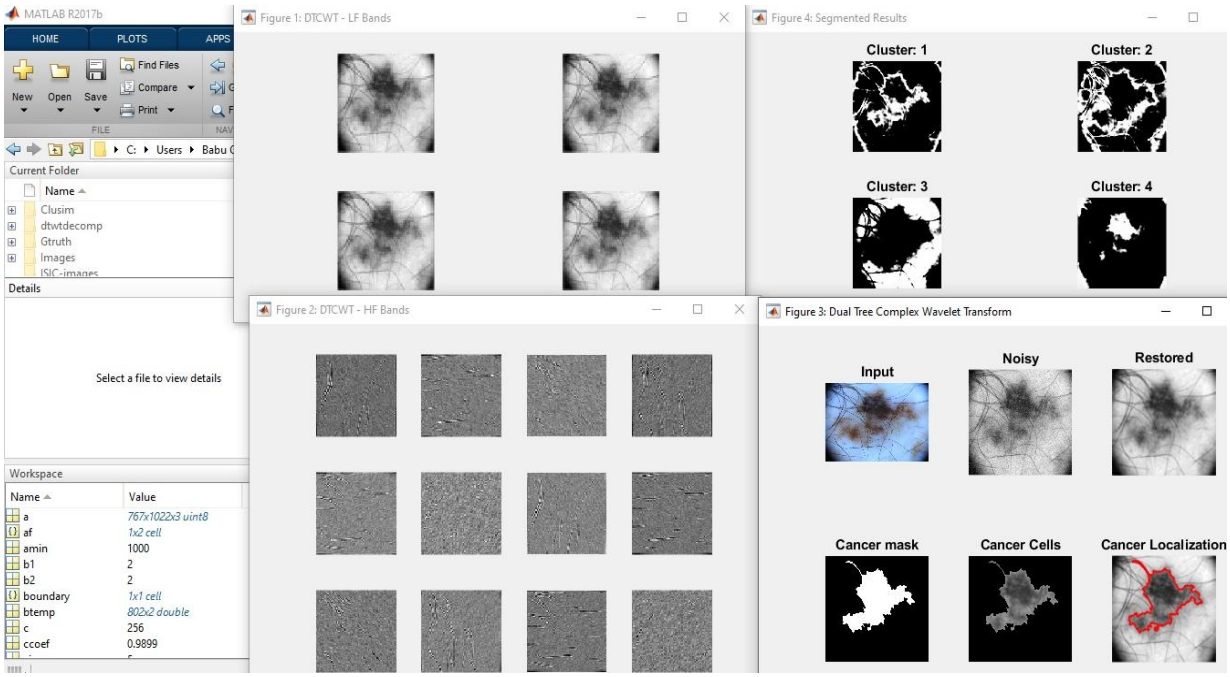

Fig 17: A noisier sample signal and the clustered output

We also measured the different output indicators used to detect the noisy image. The efficiency measurements contain Correlation Coefficient, Sensitivity, Structure Similarity Index, PSNR Values, Number of Abnormal Cells, Skin Lesion Area, Specificity, Accuracy, Image Enhancement Factor, Percentage Residual Difference and RMS Error. Figure 18 displays the segmentation process findings though for smaller tumor edges.

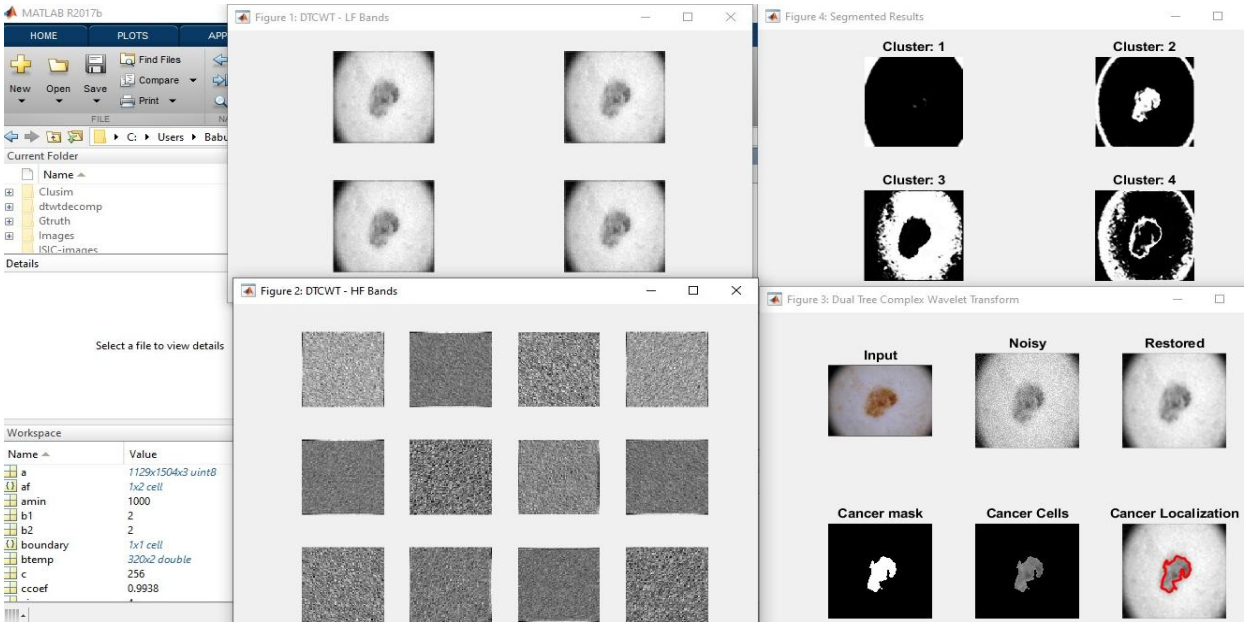

Fig 18: A smaller skin lesion region filtering and segmentation results

Annals of R.S.C.B., ISSN:1583-6258, Vol. 25, Issue 5, 2021, Pages. 743-768
Received 15 April 2021; Accepted 05 May 2021.

Images / Parameters	RMS error	PSNR in dB /100	Percentage Residual Difference	Image Enhancement Factor / 100	Correlation Coefficient	Structure similarity index	Abnormal cells /1000	Cancer area in mm^2 / 100
Image 1	5.6315	0.4062	0.9975	0.7678	0.994	0.9242	2.168	0.1229
Image 2	5.6143	0.4063	1.0203	0.7705	0.9975	0.884	6.249	0.2086
Image 3	5.628	0.4062	0.9968	0.7681	0.9987	0.9164	10.387	0.3769
Image 4	5.5037	0.4072	0.9789	0.8047	0.9897	0.8311	11.815	0.2869
Image 5	5.5925	0.4065	1.011	0.7799	0.9961	0.8497	8.184	0.4432
Image 6	5.6207	0.4063	1.003	0.7708	0.9938	0.9089	3.954	0.1660
Image 7	5.6199	0.4063	1.023	0.7713	0.9968	0.8871	12.407	0.2940
Image 8	5.1507	0.4101	0.9123	0.8244	0.9922	0.8626	15.731	0.3311
Image 9	5.6328	0.4062	0.997	0.7693	0.997	0.9067	15.460	0.3282
Image 10	5.5988	0.4064	0.991	0.7752	0.9931	0.8839	15.251	0.3260

Table 1: Performance metrics for filtering 10 sample images

We also displayed the output metrics chart for reference 12 images to see attributes distribution over various images of skin lesions as seen in figure 19.

Annals of R.S.C.B., ISSN:1583-6258, Vol. 25, Issue 5, 2021, Pages. 743-768
Received 15 April 2021; Accepted 05 May 2021.

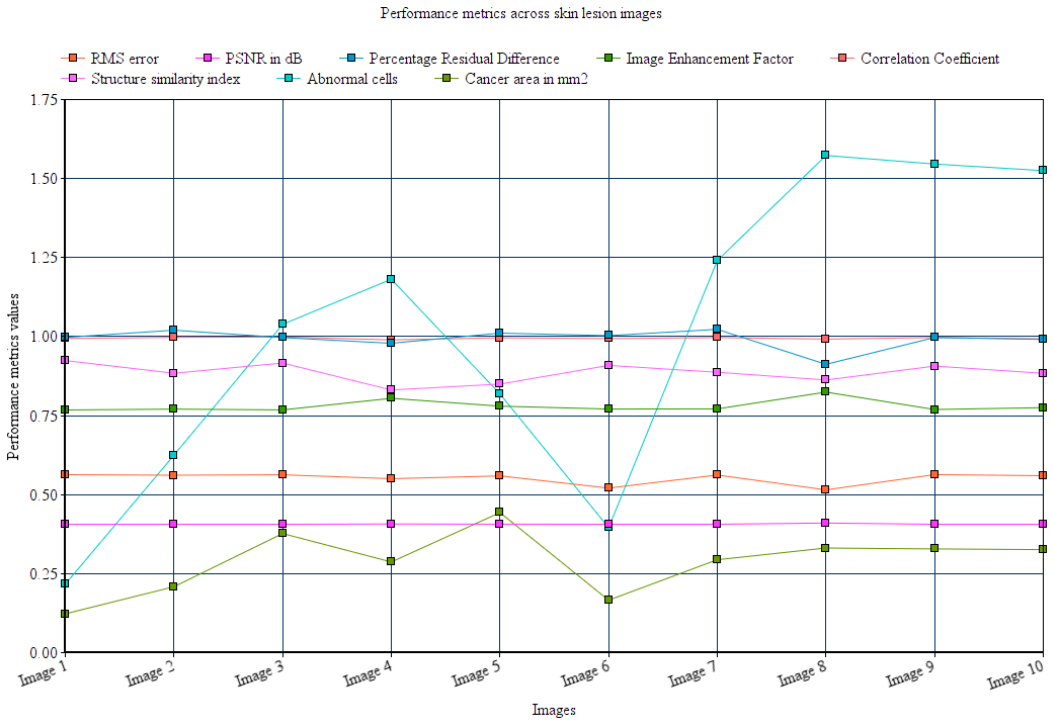

Fig 19: Performance metric plot across different skin lesion images

Figure 20 demonstrates some noisy example of a sample outcome. The groups are segregated and preserved more specifically to classify the origin of the skin tumor.

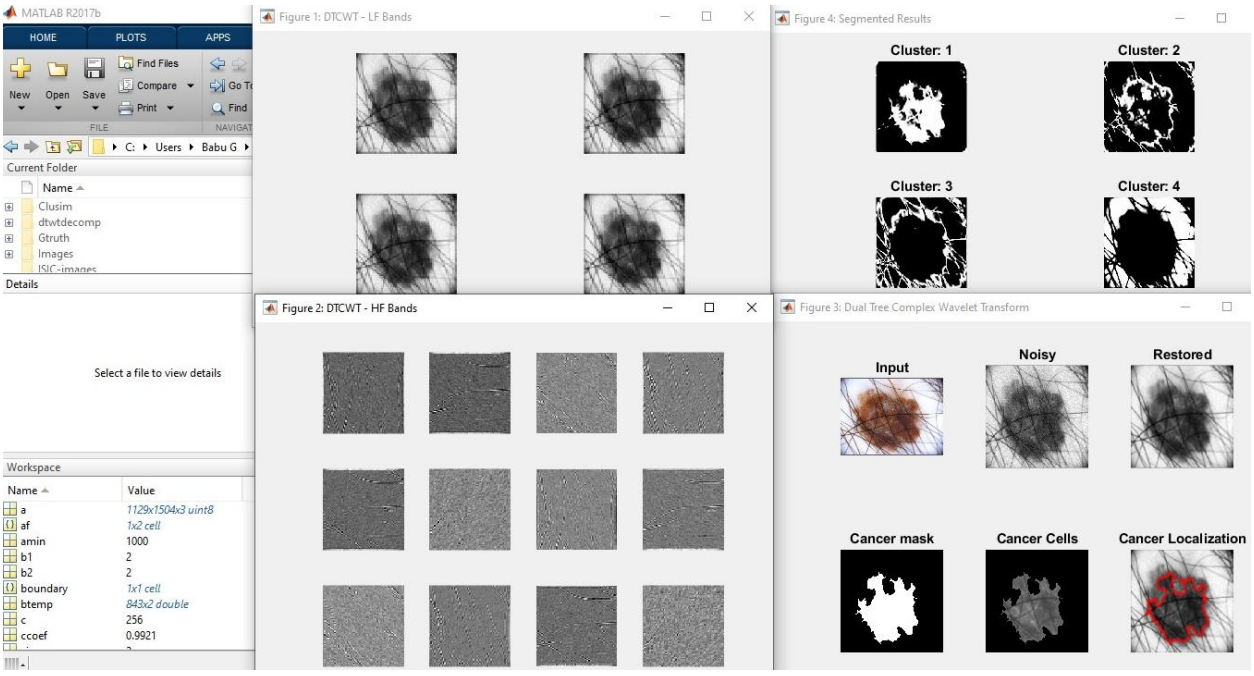

Fig 20: Performance metric plot across different skin lesion images

Annals of R.S.C.B., ISSN:1583-6258, Vol. 25, Issue 5, 2021, Pages. 743-768
Received 15 April 2021; Accepted 05 May 2021.

The results clearly show the proposed method produced good outcomes comparably existing systems. It is represented in table 2.

Images / Parameters	Image 1	Image 2	Image 3	Image 4	Image 5	Image 6	Image 7	Image 8	Image 9	Image 10
Sensitivity	78.53	97.53	97.53	90.04	94.83	89.10	93.36	93.17	96.48	95.23
Specificity	99.83	99.93	99.64	98.89	97.65	99.83	98.74	98.63	99.73	97.20
Accuracy	98.98	99.69	98.97	97.20	96.41	99.12	97.71	97.29	98.94	96.76

8. Conclusion

The method used throughout the proposed method has proved to have been efficient or simple procedures of eliminating noise from the clinical image and identifying the skin tumor and measuring the region of the tumor region. A method known as the dual-tree complex wavelet transform is included in the proposed method to turn the clinical image into a frequency field.This DTCWT is worthy of even more integration boundaries in clinical images, since it has 14 high-frequency sub-bands and two low-frequency sub-bands that are greater than the WT and Curvelet.The test results demonstrated that the DTCWT reliably provides the maximum PSNR, system resemblance Index, and biologically active natural Object coefficient of correlation, etc and greatly decreases RMSE and PRD relative to the Curvelet and Wavelet transformation. Often, the WT dual tree structure works well in tumor detection.For de-noising, the Bivariate Shrinkage and Speckle Reducing Anisotropic Diffusion Filter are known to be the efficient process. Computational Fuzzy C often denotes clustering and has proved to be the effective method in segmentation. Furthermore, the Distance in the tumor region is determined on the basis of the photographs collected from a patient's regular scans.For the future, that tumor impact of tumor nature will be determined specifically by assessing the region in which the tumor is produced throughout the skin. For the purpose of improvement, photographs should be taken from the same area of operation, and thus it is easier which technology seems to be best for which specific technique. Modern filtering strategies can be combined with other design to get the best result.Optimizing different segmentation and de-noising methods could be done to minimize the computational complexity. In comparison, various types of noise-based algorithm are used for many de-noising systems and can be contrasted with the output of those approaches.

Reference

1. Ahmed Elazab, Ahmed M. Anter, Hongmin Bai, Qingmao Hu, Zakir Hussain, Dong Ni, Tianfu Wang, Baiying Lei, an optimized generic cerebral tumor growth modeling framework by coupling biomechanical and diffusive models with treatment effects, applied Soft Computing,Volume 80,Pages 617-627,ISSN 1568-4946, 2019.

2. okulalakshmi, A., Karthik, S., Karthikeyan, N. et al. ICM-BTD: improved classification model for brain tumor diagnosis using discrete wavelet transform-based feature extraction and SVM classifier. Soft Computing, 17 June 2020.
3. Choi, H.; Jeong, J.: 'Despeckling algorithm for reducing speckle noise in images generated from active sensors', Electronics Letters,IET Digital Library, June 2020.
4. Saeedzarandi, M., Nezamabadi-pour, H. &Jamalizadeh, A. Dual-Tree Complex Wavelet Coefficient Magnitude Modeling Using Scale Mixtures of Rayleigh Distribution for Image Denoising. Circuits Syst Signal Process 39, 2968–2993, 2020.
5. X. Zhang, W. Pan, Z. Wu, J. Chen, Y. Mao and R. Wu, "Robust Image Segmentation Using Fuzzy C-Means Clustering With Spatial Information Based on Total Generalized Variation," in IEEE Access, vol. 8, pp. 95681-95697, 2020, doi: 10.1109/ACCESS.2020.2995660.
6. Yiming Tang, Fuji Ren, WitoldPedrycz,Fuzzy C-Means clustering through SSIM and patch for image segmentation,Applied Soft Computing, Volume 87,105928,2020.
7. Lenin Fred A., Kumar S.N., Padmanabhan P., Gulyas B., Kumar H.A. (2020) Analysis of Segmentation Algorithms for Detection of Anomalies in MR Brain Images. In: Jayakumari J., Karagiannidis G., Ma M., Hossain S. (eds) Advances in Communication Systems and Networks. Lecture Notes in Electrical Engineering, vol 656, June 2020.
8. hi Li, ZhenhongJia, luyangliu, Jie Yang, Nikola Kasabov,A method to improve the accuracy of SAR image change detection by using an image enhancement method,ISPRS Journal of Photogrammetry and Remote Sensing, Volume 163, 2020.
9. Raath, Kim and Ensor, Katherine B. and Scott, David W. and Crivello, Alena, Denoising Non-stationary Signals by Dynamic Multivariate Complex Wavelet Thresholding, January 30, 2020.
10. L. Sathish Kumar and A. Padmapriya, "Evidence based subsequent disease extraction from EMR Health Record by Grade Measure," 2016 Online International Conference on Green Engineering and Technologies (IC-GET), Coimbatore, 2016, pp. 1-5, doi: 10.1109/GET.2016.7916771.
11. L. KUO, B. Wang, N. Guo, K. YU, C. Yu and C. Lu, "Enhancing SNR by Anisotropic Diffusion for Brillouin Distributed Optical Fiber Sensors," in Journal of Lightwave Technology, doi: 10.1109/JLT.2020.3004129, 2020.
12. Chang Liu, Xiaodi Wang, Yuan Huang, Youbo Liu, Ran Li, Yang Li, Junyong Liu, A Moving Shape-based Robust Fuzzy K-modes Clustering Algorithm for Electricity Profiles, Electric Power Systems Research, Volume 187, 2020.
13. Xu, Huan Chun et al. 'The Image Segmentation Algorithm of Colorimetric Sensor Array Based on Fuzzy C-means Clustering'. 1 Jan. 2020 : 3605 – 3613.
14. Sathish Kumar Lakshmanan, Efficient Approach Of Memory Glow Method For Find The Misplaced Items, International Journal of Scientific & Technology Research, 9:4, 3563-3567, April, 2020.

15. S. Roy and P. Maji, "Medical Image Segmentation by Partitioning Spatially Constrained Fuzzy Approximation Spaces," in IEEE Transactions on Fuzzy Systems, vol. 28, no. 5, pp. 965-977, May 2020, doi: 10.1109/TFUZZ.2020.2965896.
16. Pritpal Singh, A neutrosophic-entropy based adaptive thresholding segmentation algorithm: A special application in MR images of Parkinson's disease, Artificial Intelligence in Medicine, Volume 104, 2020.
17. P. K. Mishro, S. Agrawal, R. Panda and A. Abraham, "A Novel Type-2 Fuzzy C-Means Clustering for Brain MR Image Segmentation," in IEEE Transactions on Cybernetics, doi: 10.1109/TCYB.2020.2994235.
18. Ronghua Shang, Chen Chen, Guangguang Wang, Licheng Jiao, Michael AggreyOkoth, RustamStolkin, A thumbnail-based hierarchical fuzzy clustering algorithm for SAR image segmentation, Signal Processing, Volume 171, 2020.